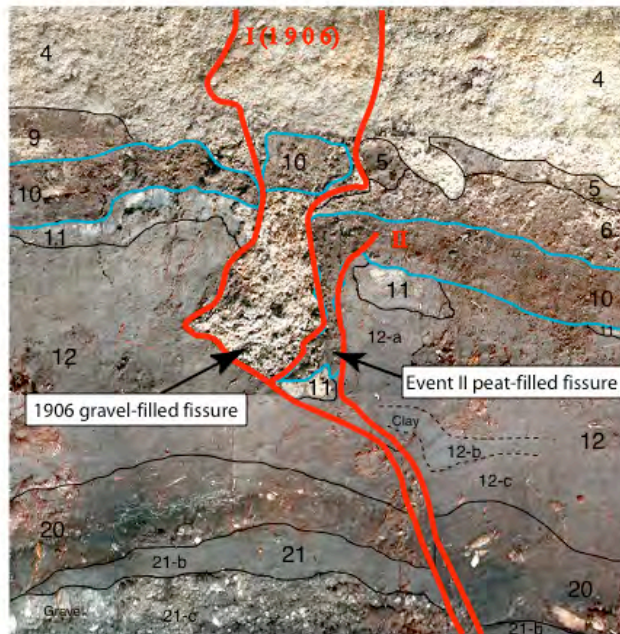


U.S.G.S. Award No. NEHRP 01HQGR0194
FINAL TECHNICAL REPORT

**Determination of a High Resolution Paleoseismicity
Chronology for the Northern San Andreas Fault at the
Vedanta Marsh Site, Marin County, CA**

*Tina M. Niemi, Ph.D.
Hongwei Zhang*

Department of Geosciences
University of Missouri - Kansas City



“Research supported by the U.S. Geological Survey (USGS), Department of the Interior, under USGS award number NEHRP 01HQGR0194 - University of Missouri-Kansas City. The views and conclusions contained in this document are those of the authors and should not be interpreted as necessarily representing the official policies, either expressed or implied, of the U.S. Government.”

**Determination of a High Resolution Paleoseismicity Chronology for
the Northern San Andreas Fault at the
Vedanta Marsh Site, Marin County, CA**

Tina M. Niemi, Ph.D.
Hongwei Zhang
Department of Geosciences
University of Missouri-Kansas City
5110 Rockhill Road, Kansas City, MO 64110
Tel: (816) 235-5342; Fax: (816) 235-5535
niemit@umkc.edu

Technical Abstract:

At the Vedanta marsh site located in Olema, California, a well-defined stratigraphy and abundant *in-situ* organic material allow the determination of the first long, high-resolution multiple event record for the north coast segment of the San Andreas fault. During the 1906 San Francisco earthquake, the ground ruptured along the northeastern edge of the Vedanta marsh where historical offset measurements near the site were about 5m. One large 20m x 9m trench with sloped sides (V-ditch) and eight backhoe trenches were excavated across the fault during the 2001 and 2002 field seasons. The main fault zone consists of a 2-m-wide zone of upward-branching fault splays within the marsh stratigraphy. A secondary fault zone located 5m to the east juxtaposes older sediment (>18 ka) against colluvium in apparent normal separation. We exposed a 4 m section consisting of eight major peat layers interbedded with fluvial gravel and marsh clay and silt that interfinger eastward with colluvial gravels. A clear, vertical transition from predominantly fine-grained marsh deposits to coarse-clastic sediment occurs at a depth of approximately 1 m and is probably caused by historical logging and landuse changes in the watershed. AMS radiocarbon dating of more than 70 samples of peat, macrofossils, and charcoal collected throughout the section indicate that the base of the exposed section is about 2500 yr B.P.

Based on outward-splaying, upward fault terminations and fault fissure fills, we identified evidence for eleven earthquakes in the 4-m-thick stratigraphic section exposed at the Vedanta marsh site. The upper four faulting events are best constrained because they have been mapped in six other trenches. Event I, the 1906 earthquake, ruptures the upper fluvial and colluvial gravels. The penultimate event (Event II) appears to offset the upper peat (unit 10, ca. 160-220 yr BP). Event III occurs after the deposition of peat layer 20 (ca. 600 yr BP) and terminates in the base of the silty clay layer 12. Layer 12 is a thick layer found on both the east and west sides of the San Andreas fault and represents a notable expansion of the standing water. Event IV forms a well-defined v-shaped fissure that is clearly capped by gravel and clay above peat unit 30 (ca. 1030 yr BP). Events V and older events were only exposed in the V-Ditch exposure. Event V is a fissure fill that occurred when peat layer 30 was at the surface. Event VI forms a couple of small fissures that disrupts the base of the organic layer 40 (1205 yr BP). Event VII

occurs when peat layer 50 was at the surface (1300 yr BP). Event VIII is seen as a peat-filled fissure and a truncation of peat layer 60. Event VIII terminates below organic-rich layer 55 (1515 yr BP). Event IX is below peat layer 60 (2000 yr BP); Event X is between layers 60 and 70; and Event XI is below peat layer 70 (2500 yr BP). Peat layer 80 has a date at about 2800 yr BP. These data clearly indicate that the actual repeat time between each surface faulting event is irregular, ranging from 100 years to 400 years.

Non-Technical Abstract:

At the Vedanta paleoseismic site located in Olema, north of San Francisco, well-defined stratigraphy and abundant *in situ* organic material allow the determination of the first long, high-resolution multiple-event earthquake record for the north coast segment of the San Andreas fault. Trench excavations across the fault show a 2-m-wide main fault zone of upward-branching fault splays within the marsh. Eleven earthquakes including the great 1906 San Francisco earthquake appear to have ruptured this portion of the San Andreas fault over the past 2500 years. Correlation between trenches and radiocarbon dates indicates a range of recurrence intervals between paleoearthquakes. Determining the timing of past San Andreas fault earthquakes has great significance for the long-term seismic hazards of the densely populated San Francisco Bay region. The results of this research will be used to test earthquake rupture models of the San Andreas fault and to improve the earthquake probability estimates published by the U.S. Geological Survey. The goal of these earthquake probability estimations is to increase public preparedness and to reduce the loss of lives and property in future earthquakes.

Determination of a High Resolution Paleoearthquake Chronology for the Northern San Andreas Fault at the Vedanta Marsh Site, Marin County, CA

*Tina M. Niemi, Ph.D.
Hongwei Zhang
Department of Geosciences
University of Missouri-Kansas City*

Introduction

The great San Francisco earthquake of April 18, 1906, was generated by 470-km-long rupture of the northern San Andreas fault (Lawson, 1908). The 1906 coseismic slip was >5m north of San Francisco and <3 m on the San Francisco Peninsula and to the south (Lawson, 1908; Thatcher *et al.*, 1997). At the latitude of San Francisco, the northern San Andreas fault slip rate of 24 mm/yr (Niemi and Hall, 1992) is partitioned between the San Gregorio fault and the San Francisco Peninsula San Andreas fault (Fig. 1). These data in conjunction with a historical earthquake in 1838, with a probable epicenter on the San Francisco Peninsula (Topozada *et al.*, 1981; 2001; Topozada and Bortugno, 1998), have lead many scientist to conclude that the northern San Andreas fault north and south of the Golden Gate behave as different fault segments. However, since the historical data do not extend over a complete earthquake cycle, little is known about the long-term fault behavior of the northern San Andreas fault.

Earthquake hazard assessments rely on variously proposed fault behavior models. For the northern San Andreas fault, the Working Group on California Earthquake Probabilities (WGCEP, 2003) used several models ranging from less constrained poissonian to more constrained characteristic models where slip distribution along the fault length is assumed to remain the same through repeated cycles (Schwartz and Coppersmith, 1984). Recent seismic source characterization efforts for the San Andreas fault and San Gregorio fault have tried to factor different earthquake rupture scenarios into the probabilities (WGCEP, 2003; Zoback and Schwartz, 1999). In addition to the characteristic earthquake model, both a random (floating) earthquake model and several non-1906 segment models were evaluated. Few constraints limit the various models. Critical physical paleoseismic data (earthquake repeat time and slip-per-event) for the northern San Andreas fault must be collected in order to discriminate between alternative fault behavior models.

Earthquake recurrence records are the most fundamental data sets with which all fault behavior models must be reconciled. However, data that constrain the recurrence behavior for the San Andreas fault are surprisingly sparse, especially considering that this is the most studied and modeled fault in the world. On the northern San Andreas fault, the Vedanta site is one of only a very few sites that has shown the potential to provide a comparable high-resolution record for earthquake recurrence over the past 2500 years. Promising new data from turbidite records off the California continental margin may provide an independent record of earthquake recurrence (Goldfinger *et al.*, 2003).

The main objective of this research is to obtain a high-precision, event-by-event chronology of ground-rupturing earthquakes that is confirmed in multiple trench

exposures across the northern San Andreas fault. The anticipated outcome of this research is a better definition of the earthquake cycle in the San Francisco Bay Area. The Bay Area straddles the Pacific-North American Plate boundary where tectonic strain is distributed across several faults including the San Gregorio fault to the west and the Hayward-Rodgers Creek, Calaveras, Greenville, and Concord faults to the east of the San Andreas fault. The majority (>50%) of the plate motion in the region is concentrated on the San Andreas fault. Major earthquakes on the San Andreas fault apparently drive the Bay Area seismicity based on a post-1906 stress shadow and period of seismic quiescence (Harris and Simpson, 1998).

Determining the timing of past San Andreas fault earthquakes has great significance for the long-term seismic hazards of the densely populated San Francisco Bay region. The results of this research will be used to test earthquake rupture models of the San Andreas fault and to improve the earthquake probability estimates published by the U.S. Geological Survey (WCEP, 2003). The goal of these earthquake probability estimations is to increase public preparedness and to reduce the loss of lives and property in future earthquakes. This research directly addresses Element III of NEHRP research priorities to understand earthquake occurrence and effect through the determination of paleoearthquake chronologies.

Geologic Setting and Previous Research

The northern San Andreas fault in Marin County forms a linear topographic depression that extends from Bolinas Lagoon in the south to Tomales Bay in the north (Fig. 2). Within the middle of the fault valley are remnants of deformed Upper Pleistocene fluvial to lacustrine sediments [Olema Creek formation (Qoc)] and fluvial terraces [Quarry fan deposits, Qqf (~30–18 ka) and Older Quaternary alluvium, Qoa (>30 ka) deposits] that form a medial ridge (Hall and Hughs, 1980; Grove *et al.*, 1995). The Vedanta marsh paleoseismic site is located on the Vedanta Retreat property in Olema. Here, the 1906 trace of the San Andreas fault lies between a marsh and a ridge of late Quaternary fluvial terrace deposits (Quarry fan; Qqf) (Fig. 2). The marsh formed as a ponded drainage, blocked at its north end by the Bear Valley Creek fan and at its south end by the Gravel Creek fan.

Several tectonically disrupted drainages are apparent in the study area. Bear Valley Creek is deflected northwestward along the San Andreas fault trace and eventually flows to the Tomales Bay. However, it is clear that this stream once flowed across the medial ridge through the Water Gap and joined Olema Creek on the east side of the valley (Niemi, 1992; Grove and Niemi, 2005) (Fig. 2). The current course of Gravel Creek is an artificial drainage that flows along the western and northwestern margin of the marsh and through the Water Gap. During the Holocene, Gravel Creek built a fan across the southwestern portion of the marsh. At least one channel of Gravel Creek flowed through a gap in the medial ridge (now the Wind Gap). It was then diverted northwestward along the fault trace. Other channels drained across the Vedanta marsh in this aggrading environment throughout the Holocene.

The San Andreas fault at this site was previously studied as part of a Ph.D. dissertation (Niemi, 1992). Channel deposits at the south end of the marsh within the Gravel Creek alluvial fan and the Vedanta wind gap provided piercing point data for calculation of a minimum, late Holocene slip rate of 24 ± 3 mm/yr (Niemi and Hall,

1992). The study also established that the stratigraphic sequence at the Vedanta marsh site contained fine-grained, organic-rich sediment that would have a high probability of yielding additional paleoseismic data. Even though several trenches excavated across the fault showed evidence for prehistoric earthquakes, the limited number of radiocarbon dates prevented the determination of a high-resolution event chronology. Furthermore, stratigraphic layers and event horizons were not correlated between trenches in the Niemi (1992) study.

During the Fall of 1998 as part of the Bay Area Paleoseismic Experiment (BAPEX), two trenches were excavated across the San Andreas fault and five sediment cores were extracted from the Vedanta Marsh (Niemi *et al.*, 1999; Generaux *et al.*, 2002). Trench VT-1 was re-excavated at its previous location (Trench 12; Niemi, 1992) to a depth of 1.7m. A second, 10-m-long by 2.0 m deep trench (VT-2), was excavated approximately 17 m to the northwest of VT-1 (Fig. 3). High water-table conditions made trench logging difficult. Water was continuously pumped from the trenches using a sump pump powered by a generator. Water continued to pour out of the sides and bottom of the trench. Because the walls never dried out in either trench and the bottom of VT-2 was narrow and hand-dug, some stratigraphic relationships remained uncertain. However, our 1998 investigations showed that the marsh stratigraphy in the two trenches (VT-1 and VT-2) excavated about 20m apart could be successfully correlated.

This report covers two seasons of excavation conducted at the Vedanta paleoseismic site during August- November 2001 and June-August 2002 under the NEHRP contract number 01HQGR0194. The success of the recent research efforts is marked by a new strategy to dewater the site. In August 2001, we used a track excavator to open a 4-m deep ditch with sloped sides (hereafter referred to as the V-ditch). The V-ditch is a 9-m-wide and 20-m-long trench that crosses the fault (Fig. 3). Originally, the V-ditch continued in an L-shape, parallel and west of the fault for other 30 m. The V-ditch was excavated to intercept the water from a target area northwest of the excavation. The initial purpose of digging the V-ditch was for de-watering the study site in the marsh. Surprisingly, this V-ditch, especially its north wall, preserved the most complete and continuous record of earthquakes yet recovered at the Vedanta site. Its large dimensions also were the key to drying the site and allowing for the recovery of the long paleoearthquake chronology that we have documented.

In addition to the V-ditch, in 2001 we also logged four 2- to 3-m deep trenches excavated across the fault (Trenches VT-1, VT-3, VT-4, and VT-5; Fig. 3). In the 2002 field season, Trenches VT-1 and VT-3 were re-opened. Two new, rather short and shallow trenches (Trenches VT-6 and VT-7) were excavated across the fault trace to confirm the event horizon for the penultimate earthquake. Also, Trench VT-8 was excavated at the bottom of the V-ditch across the fault zone in an attempt to extend the length of the event record another 500 years. Several phases of logging were also conducted as the walls were peeled back on the south wall of VT-1, north wall of VT-3, and both the south and north wall of V-ditch in order to eliminate any ambiguities of the event horizons and to collect additional data for all of the individual events.

At the end of the 2001-02 seasons and the NEHRP 01HQGR0194 grant, we had developed a generalized stratigraphic sequence that can be used to correlate event stratigraphy between the trenches. We also identified ten pre-1906 earthquakes based on evidence of outward-splaying, upward fault terminations and fissure fills. Stratigraphic

records of the four most recent earthquakes were recovered in the shallower trenches. Earlier events were exposed in the one deep V-ditch exposure and are confined between the section dated to approximately 1000 A.D. to 900 B.C. Many of the trenches did not have evidence for all of the earthquakes, but when combined they strongly support the youngest five events. In the next section, we discuss the marsh sediment stratigraphy, event stratigraphy, and the model for determine ages of the sedimentary layers and paleoearthquakes.

Marsh Stratigraphy

Constraints on active deformation of the Vedant marsh deposits and the nature of their contact with Upper Pleistocene sediments (Qoa and Qqf) were obtained by studying paleoseismic trenches excavated perpendicular to the SAF. The late Holocene stratigraphic section exposed in the upper four meters of the Vedanta marsh can be divided into four main facies—marsh, fluvial gravel, colluvial gravel, and anthropogenic gravel facies.

The marsh facies consists of fine-grained sediments that alternate between organic-rich sediment, clay, and silt layers. We numbered each organic horizon (including peats and wood-rich clay) by units of 10 starting at the top of the section. There are eight organic horizons (units 10-80). Upon further examination of the section, several intermediate organic horizons were recognized and labeled by units of 5 (including layer 35, 45, and 55). These “peats” contain both decayed vegetative mats formed *in situ* and organic debris derived from the adjacent uplands and medial ridge. Acorns, pinecones, oak leaves, branches, and tree fragments are preserved in these layers. The organic horizons are sometimes associated with charcoal, wood ash, *in situ* burns, and oxidized sediment patches, and burnt logs. The thickness of each marsh unit generally ranges from 15 to 25 cm. The units generally pinch out eastward where the marsh deposits interfinger with ridge-derived colluvial gravels. The marsh sequence comprises about four-fifth of the section and is characterized by continuous subaqueous deposition. The contact between texturally different layers (clay, silt, silty clay, or clayey silt) is generally gradational. The upper boundary of the organic horizons tends to be comparatively sharp.

Interfingering with the marsh facies are fluvial and colluvial gravels. Wedge-shaped gravelly clay deposits thicken toward the east. The colluvium is composed of granules, pebbles, and cobbles of predominantly siliceous shale (Monterey Formation) clasts within a matrix of clay. These clayey gravel layers represent colluvium shed from the adjacent ridge of Upper Pleistocene alluvial fan sediments that were deposited into the fine-grained sediment of the marsh. The fluvial deposits at this site have limited lateral continuity and are confined to channels. Fluvial gravels and sands are distinguished by the lack of matrix and the clear lenticular boundaries of the channel margins.

An approximately one-m-thick anthropogenic gravel facies caps the entire sequence. This upper clastic sequence is divided into layers 1-8. Layers (1-3) consist of a modern fill and colluvium produced by mechanized equipment. These layers are post-1906, i.e. they are not faulted by the 1906 earthquake. The fill is soft, dark gravelly clay or clayey gravel with dense array of roots. Artifacts such as barbed wire, square nails, fence posts, and slabs of road pavement were found in this layer. Along the eastern edge

of the marsh, near the west slope of the medial ridge, remnants of a buried soil developed on the colluvium are preserved. Underlying these layers are recent channel deposits (layers 4-5) that in places have distinct graded bedding, cross stratification, sand lens, and iron-oxide-coated pebbles. In other places, the gravel is mixed with a matrix of fine-grained sediment (layer 6) and is apparently bioturbated and colluvial in nature. The base of layer 6 is erosional. The shift from fine-grained marsh sedimentation toward coarse-clastic sedimentation at this location signals an environmental change possibly triggered by the regional deforestation and denudation caused by the arrival of European settlers and loggers. Efforts to drain the marsh over the past 150 years have also lowered the water table about 1.5 m (Niemi, 1992). Historical erosion, channel incision, and increased sedimentation rates have been documented for this region (Niemi and Hall, 1996). Burrows and deep erosional contacts are only seen in the upper 1.5 m of section (units 12 and younger) and are related to the human-induced lowering of the water table.

Burn and ash layers have a unique color that is distinct in the exposures. These burn layers are included in the generalized stratigraphic column and description. However, we only name the uppermost one as an independent unit (layer 11) because it is extensive and can be correlated across the trench exposures. Other burn layers are either so limited in extent or only observed in lower part of V-Ditch that they cannot be correlated as a unique layer.

The definition of a unified stratigraphic sequence that can be correlated between exposures is extremely important because earthquakes cannot be dated directly. Age constraints on paleoearthquakes are derived from dating the last layer disrupted by an earthquake (the event horizon), and the youngest layer to cap the event. A composite section showing all stratigraphic units and sub-units of the Vedanta marsh sequence is shown diagrammatically in Figure 4. Every unit is not present in each trench exposure.

Co-seismic Deformation and Subsidence

Trenches excavated perpendicular to the trend of the San Andreas fault exposed a 6-m-wide fault zone at Vedanta marsh. This fault consists of a narrow, 2-m-wide zone of upward-branching fault splays within the marsh, and a secondary fault zone that juxtaposes older alluvium [Qqf (~30–18 ka) and Qoa (>30 ka)] against colluvium in apparent normal separation.

Niemi (1992) used archival data, including historical descriptions, sketches, and photographs of the 1906 rupture, to precisely locate the fault trace and to document the style of coseismic deformation at the marsh (Gilbert, 1907a; 1907b; Notebooks at U.S.G.S. archive, Denver; J.C. Branner photography, Stanford Univ. Archive). In addition to fault rupture, active tectonic subsidence of the Vedanta marsh was observed at the time of the 1906 earthquake (Lawson, 1908), when a lane of water ponded against the rupture trace. The 1906 faulting through the marsh was on a straight, narrow trace near the western base of the Quarry fan ridge and on a sidehill bench trace on the ridge southeast of the marsh (Fig. 2). The secondary coseismic geomorphic changes at this site included: (1) a zone of secondary cracking 3.0 to 4.5 m wide, (2) local subsidence that temporarily reversed the flow of Gravel Creek and ponded water 70 cm deep along the fault trace, and (3) slump failure along the west side of the ridge that caused the embankment of a dirt road to slide into the marsh. Trenching in the wind gap area at the

south end of the Vedanta marsh also confirmed the existence of localized subsidence along the 1906 fault trace (Niemi and Hall, 1992).

The rate of differential subsidence across the active 1906 trace of the San Andreas fault can be estimated by using the top of peat layer 60 as a marker (Fig. 5). The top of peat 60 has an apparent vertical separation across the fault of 90 cm. Radiocarbon analysis on organic material from the layer yielded a radiocarbon age of ca. 2100 yr B.P. These data suggest a 0.4 mm/yr tectonic subsidence rate. Successively younger peats have progressively less apparent vertical separation. The calculated subsidence rate for peat 60 is less than the sediment accumulation rate calculated for the 3.3-m-thick section of marsh deposits. This suggests that the amount of vertical separation may include apparent offset due to lateral displacement of units, and thus may not represent the full tectonic subsidence. The rate of 0.4 mm/yr is comparable, however, to the late Quaternary subsidence rates for San Francisco Bay of approximately 0.2-0.4 mm/yr (Atwater *et al.*, 1977). These data suggest that the ratio of vertical slip to strike slip across the 1906 trace of the SAF at this site is relatively small. Subsidence is probably accommodated on the secondary fault that juxtaposes colluvium and interfingering marsh sediment against Qqf and Qoa sediment. The amount of tectonic subsidence on this fault cannot be estimated due to a lack of stratigraphic match across the structure.

Event Stratigraphy

Trenches excavated across the San Andreas fault at the Vedanta site reveal stratigraphic data for both historic and prehistoric earthquakes. Evidence for eleven earthquakes (seismic events) was identified in the 4-m-thick Vedanta stratigraphic section exposed in the V-Ditch (Fig. 6). The upper four faulting events are best constrained at the Vedanta site because they have been mapped in seven other trenches. Because most of the trenches were not deep enough to expose event evidence for earlier earthquakes, Event V to Event XI were identified mainly from the V-ditch exposures, especially on the north wall. The main role of V-ditch was to intercept the groundwater coming from south. Continuous seepage of groundwater from the south wall caused this exposure to collapse, especially within the fault zone. Due to the lack of a stable, continuous, flat and deep section, and the wet conditions, stratigraphic relationships on the south wall of the V-ditch had some uncertainty.

The earthquake evidence is based on upward fault terminations, fissure fills associated with surface rupture, fault-scarp-derived colluvial-wedge deposits, soft-sediment deformation such as folding and liquefaction features due to strong ground shaking, unconformities or abrupt changes in deformation between stratigraphic units, rotated and truncated blocks along the fault. Upward fault termination do not always provide reliable information on the stratigraphic position of the ground surface at the time of faulting event, because even within well-stratified deposits, fault strands (especially subsidiary fault strands) do not always terminate upward at a consistent stratigraphic level in different exposures (*e.g.*, Bonilla and Lienkaemper, 1990; Fumal *et al.*, 1993; Weldon *et al.*, 1996). Therefore, our event chronology is based largely on the more reliable fissure fill evidence seen in the Vedanta exposures.

The “event horizon” (or earthquake horizon) is the layer that represents the ground surface at the time of an earthquake. One way to identify the event horizon is to bracket the fault strand between the highest faulted stratum and the lowest, well-defined

stratum that caps the fault, and is clearly not faulted. Event horizons are also identified based on fissure fill material. A fissure is the upward branching of the fault as it reaches unconfined surface pressures. Blocks of material within the upper 0.2-0.5 m of the surface become sliced, faulted, folded, entrained, and fall into the ground rupture fissure. Layers that are deposited after the earthquake cap the fissure. The most conclusive evidence for any single paleoearthquake is multiple lines of evidence from several different trench exposures.

A summary of the stratigraphic and structure data for each faulting event at the Vedanta site follows. These data were used to develop the earthquake chronology of the site. We have labeled the earthquakes with Roman numerals. The events are numbered sequentially from youngest to oldest with Event I representing the 1906 earthquake (i.e. the most recent event). Higher Roman numerals indicate older earthquakes. The summary only discusses the major evidence used to define the event horizons. Detailed information from each trench is found in Zhang (2005).

The 1906 Earthquake (Event I)

Our study shows that the ground surface at the time of the 1906 earthquake was layer 4. The stratigraphic evidence for this event horizon was documented in the north wall of the V-ditch (Fig. 5) and in the five trenches (VT-1, VT-2, VT-3, VT-6, and VT-7) to the northwest. A well-developed fissure that was filled with the upper gravel is preserved in several trench exposures (Figs. 6 and 7). The stratigraphic evidence of the 1906 event horizon is not present in the south wall of the V-ditch or in Trenches VT-4 and VT-5 that are located south of the V-ditch. The excavation of a drainage channel at this location by the landowners has removed the upper portion of the stratigraphic section.

Trenches VT-1, VT-2, and VT-3 and the V-ditch extended across the fault contact between the Upper Pleistocene fluvial deposits of the medial ridge to the east and the marsh sediment with interbedded colluvium. Detailed mapping of this contact indicated that faulting occurred on the secondary normal fault zone during the 1906 earthquake. In Trench VT-1, a gravel bed that has the same sedimentary texture and color as the gravel bed with crossing bedding above the main fault zone (layer 4) was cut by the fault with clear normal displacement. These data corroborate the interpretation of layer 4 as the event horizon for the 1906 earthquake.

Indirect evidence for the 1906 event horizon is the change in the marsh depositional environment from fine-grained to coarse-clastic sediment. Wide spread changes in hillslope erosion and basin sedimentation rates due to anthropogenic activities occurred since about the late 1850s when the area was settled by Europeans (Livingston, 1995; Niemi and Hall, 1996). In cores extracted from Bolinas Lagoon, historically introduced exotic plants (*e.g.*, *R. ascetocella*) were observed in sediment deposited around or before A.D. 1857-1859 (Knudsen *et al.*, 2002). If we assume the sedimentary environment change at the Vedanta marsh started at approximately the same time, the 1906 event horizon should be above the lower finer marsh sediments and terminate somewhere in the upper coarse gravel deposits. In other words, the lower part of the coarse gravel deposits that contain historical artifacts such as horseshoes and barbwire are involved in faulting during the 1906 earthquake.

The Penultimate Event (Event II):

Differentiation between faulting in the 1906 earthquake and the penultimate earthquake has been somewhat hampered due to various processes that have obscured the record including: 1) Disturbance by human activities such as artificial drainage system excavation and road reconstruction along the fault trace after 1906 earthquake. The drainage ditch excavated in 1948 above and near the 1906 rupture trace in places destroyed much of the uppermost section; 2) Extensive bioturbation by burrowing animals, especially along the fault zone, to a depth of about 1.5 to 2 m; 3) Erosion at the base of a channel deposit that flowed along the fault trace before and just after 1906 earthquake and removed portions of the stratigraphic record; and 4) The narrow fault zone in which 1906 earthquake may reoccupy, blur or destroy the evidence left by the penultimate event at the trench site. Overprinting by more recent faulting in relative narrow fault zone makes it difficult to decipher the record of older events, a case encountered even in paleoseismic site like Wrightwood on southern San Andreas fault (Fumal *et al.*, 2002).

Our best evidence of Event II is the fissure fill observed in trenches VT-3 and VT-6. In north wall of Trench VT- 6 (Cover photo), a compound fissure was formed by reopening the peat-filled fissure of the penultimate event and filling the overlying gravel during the 1906 earthquake. About two meters northwest in south wall of Trench VT-3 (Fig. 7), this compound fissure clearly shows the peat-filled fissure created in the penultimate event (II) that is later cut by the 1906 fault trace. Fault traces of Event II can be traced and terminated in peat layer 10 in both exposures. This relationship indicates that Event II occurred during the accumulation of the upper part of peat layer 10. Furthermore, the peat-filled fissures confirms that peat layer 10 was at the ground surface at the time of the penultimate earthquake occurred.

Deformation of the burn layer 11 adds additional evidence that there is more than one earthquake event above this stratigraphic level because units deformed only by 1906 earthquake are distinctly less deformed than units deformed by the earlier event. Ample evidence of warping (VT-3S), folding (VT-6 and VT-7), or sharp vertical displacement (VT-3N and VT-6), and abruptly lateral thickness change (VT-1S and VT-3S) of the burn layer 11 shows that the layer has undergone a more complex deformation than the overlying layers. The burn layer is a major marker bed due to its unique color. The deformation of this layer was caused by the strong earthquake shaking while it was at or near the ground surface during the penultimate earthquake. The high plasticity caused it to deform in a ductile (folds) rather than brittle manner. Shaking or agitation that caused the production of ridging and horizontal shifting of tidal mud was documented near the town of Inverness, on Tomales Bay after the 1906 earthquake (Lawson, 1908, p. 77-79).

The prominent unconformity observed in Trench VT-1 on the south wall (Fig. 8) is another strong piece of data for Event II, even though the stratigraphic section in VT-1 does not preserve the event horizon due to the erosion before the deposition of coarse gravel sediments. Layers within the main fault zone are deformed due to folding and upwarping in a moletrack. Layers 9 and 10 are absent. However, this upwarp was not the result of the 1906 earthquake because layer 5 and the bottom of layer 4 are relatively flat. The less deformed layers 4 and 5 compared with the more complex deformation of the underlying units independently confirm that these layers do indeed post-date the penultimate faulting event. Furthermore, this deformation can not be the result of Event

III because the fault cuts layer 12 in a higher stratigraphic level than evidence for Event III elsewhere at the site.

The secondary normal fault zone also preserves evidence for displacement in Event II. In Trench VT-1, the fault movement during Event II caused about a half meter vertical offset of a soil horizon that developed on the bedrock. A fissure also developed in the soil horizon and is filled with colluvium. Charcoal collected from the soil horizon yields an uncalibrated radiocarbon age of 160 ± 50 yr BP allowing an interpretation of the soil horizon to be the ground surface at the time of the penultimate event (Zhang, 2005)

The Third-Event-Back (Event III):

Event III is seen on the V-ditch north wall where a fault trace clearly cuts through the layer 20 and terminates somewhere in the layer 12 (Fig. 6). However, the determination of the exact location of the event horizon is not possible because of the homogenous sedimentary texture of the layer 12 in the V-ditch exposures. Faults are difficult to trace when they cut through the clay and silty clay layers if there are no distinct texture and color changes between the juxtaposed layers across the fault. Faults may tend to heal in clay or silty clay layers due to their high plasticity.

The best exposure of Event III is found in Trench VT-4. In the north wall of Trench VT-4, a fault splay cut across the peat layer 20 and terminates in the overlying fine gravel layer (12-e, a sublayer of layer 12) with a sharp V-shaped, fine-gravel-filled fissure. In the south wall of Trench VT-4 (Fig. 9), a fault juxtaposes different stratigraphic layers and terminates in sublayer 12-e. Both exposures clearly show that faulting in Event III does not disturb the overlying coarse gravel channel deposits (12-d). The event horizon for Event III is capped by sublayer 12-d. Evidence for Event III with sublayer 12-d as the capping layer also was recorded in trench exposures in VT-1, VT-3, VT-6, and VT-7 where the sublayer 12-d is a sandy peat or fine sand layer, probably a overbank deposit of a paleochannel. Folding of layer 20 in VT-6 on the north wall is also probably the result of Event III.

Event IV:

A large V-shaped fissure exposed in the north wall of the V-Ditch is clear evidence for Event IV (Fig. 6). The fissure is filled with blocks of layers 30 and 35 that are complexly deformed. The layer 21-c is a thin gravel bed that we interpret as colluvium derived from the medial ridge. The small gravel-filled fissures indicate that both gravel (21-c) and a lower gravel lens (sublayer 21-e) are involved in the deformation and represents the event horizon. A fault trace observed on the west side of the main fault zone also suggests the sublayer 21-c is involved in Event IV because gravels are cut and filled along the fault. The capping horizon for Event IV is the fine-grained silt of layer 21-b. A similar observation was also documented in VT-6N. The fault cuts a gravel and juxtaposes it with an underlying sublayer 21-c, but here is capped by a similar gravel. Faults that truncate the layer 22 or layer 30 and cut into sublayer 21-d have been documented in VT-1N, VT-3N, VT-3S and VT-4N (Zhang, 2005). Based on the observations from these trench exposures, the event horizon for Event IV after deposition of sublayer 21-d (a thin clay layer), but before or during the accumulation of sublayer 21-c (a thin gravel layer).

Event V:

The distinct evidence of Event V is seen in the north wall of the V-Ditch (Fig. 6). Peat layer 30 appears to be the event horizon for this earthquake on the west side of the exposure. On the east side of the exposure, a fault-bounded fissure is filled with blocks of peat 30. The faults also truncate and disturb a burn layer associated with layer 35 and juxtapose several different stratigraphic layers from layers 30 to 40. A similar type of structure is documented in the north wall of VT-1. Layer 30 is a thick, woody peat. Evidence of faults that cut and terminate in layer 30 under wood fragment can be observed on VT-1N and VT-3N. Evidence of faults that juxtapose layer 30 with different thickness and against layer 31 was also displayed on the south wall of the V-Ditch and VT-4N.

Event VI:

This event was recognized by the fault splays that truncate and juxtapose different stratigraphic layers and terminate in peat layer 40 on the north wall of the V-Ditch exposure. The peat-filled fissures allow us to interpret Event VI as occurring during the accumulation of peat layer 40. Folding of layer 42 is another indicator of Event VI. Faults that truncate and juxtapose different stratigraphic layers and terminate in peat layer 40 also displayed on the south wall of the V-Ditch and VT-1N. Several fault splays on both side of the main fault may also be attributed to this earthquake.

Event VII:

This event was only observed on the north wall of the V-Ditch. A fault trace that truncates and juxtapose layers below peat 50 appears to die out above peat 50. The strata east of the fault trace are tilted east, while west of the fault trace the strata are tilted west. This folding is confined below layer 41. A very thin white clay layer 42 appears to cap the fault trace in the the eastern exposure. These data indicate Event VII occurred when the peat layer 50 was at the ground surface. Other fault traces of this event appear to offset layer 56 with layer 41 as a capping layer. The greater apparent normal separation on top level of layer 42 compared to layer 58 may suggest an event occurred between these two layers. No evidence for Event VII was found in the south wall of the V-Ditch.

Event VIII:

Event VIII was observed on the north wall of the V-Ditch as a fault traces that truncates layers 58, 60 and 61 and juxtaposes them with layers of various thicknesses and different stratigraphic levels (Fig. 6). The fault may also disturb a burn layer and juxtapose the marsh layers with a massive clayey gravel block. The exact termination level of Event VIII in layer 58 on north wall of the V-Ditch is not well defined. However, the wedge-shaped gravelly silty clay layer 56 appears to cap the event and may represent a colluvial lens (or possible colluvial wedge) developed after this event. There is a distinctly different amount of normal separation on top level of layer 58 and layer 60 suggesting an event may have occurred in this time interval.

On the south wall of the V-Ditch (Fig. 10), this event was shown by a fault splay that terminates under a thin gravel bed in layer 58. This allows us to interpret that Event VIII occurred near the bottom of layer 58. The thin gravel bed may represent the

beginning of deposition of a colluvium from the adjacent ridge. However, culmination of deposition of colluvium was at the end of deposition of layer 58.

Event IX:

Evidence of Event IX on the north wall of the V-Ditch was identified by fault splays that truncate layer 6. Faulting in this earthquake also juxtapose marsh facies sediments with against clayey gravel (Fig. 6). The faults cut to the base of layer 60 and forma a small fissure. On the east side of the fault zone, a fault truncates underlying gravel and silty clay layers and terminated under layer 60. The termination level of this event on the south wall of the V-Ditch is somewhat uncertain. However, further excavation by hand revealed convincing evidence on DS-probe wall where a series of faults cut to the base of layer 60 with small fissure fills (Fig. 11). These data support the conclusion that Event IX occurred at the base of layer 60, or at the beginning of accumulation of layer 60.

Event X:

The two earliest events: Event X and Event XI were identified only on the north wall of the V-Ditch to the east of the main fault, no evidence was observed in the DS-probe wall. The evidence for Event X on the north wall of the V-Ditch is a fault that truncates and juxtaposes a gravel bed with a silty clay layer. The fault cuts upward and truncates peat layer 70 and is capped by the overlying gravel bed that could be the colluvial developed after this event (Fig. 6). Therefore, Event X occurred when peat layer 70 was at the ground surface, or after the deposition of layer 70.

Event XI:

This earliest event identified at the Vedanta site was shown on the north wall of the V-Ditch as faults truncated peat layer 80 and juxtaposed this layer aagainst gravel. The fault may also cut the overlying gravel, but was capped peat layer 70 (Fig. 6). So, this event occurred after layer 80 was deposited but before layer 70 and may involve the overlying gravel.

Radiocarbon Age Constraints

Our analyses combine radiocarbon age results from the 1998 BAPEX study at the site with 54 new radiocarbon dates provided from samples collected during the 2001 and 2002 NEHRP field season. Although organic materials are abundant at this marsh site, extremely careful work was taken during the sampling in order to eliminate the uncertainties caused by sedimentary reworking, fault activity, or bioturbation. Samples were collected after careful inspection based on their important relationship either to the stratigraphic boundaries or to the event horizons. The radiocarbon results yielded a large spread of ages for each layer (Fig. 12). The upper stratigraphic section contains the majority of the age determinations. More than 90 radiocarbon ages from layer 20 and above collected in different trenches were analyzed in this study. These samples consist of detrital charcoal and associated humic acid extractions, plant fragment such as twigs, leave, and wood, peat. All radiocarbon sample dates were mapped on a scatter plot of ^{14}C age verses straitigraphic level by depth (Fig. 12). The scatter plot is very helpful for identifying which samples and material types provide reliable estimates of the layer age,

and can be used to narrow down the sample dates for further OxCal radiocarbon age modeling.

We are presently still analyzing the radiocarbon data with the OxCal program to model the ages of each of the layers and events. OxCal is a Bayesian statistical computer program (Ramsey, 2005) that calibrates radiocarbon ages and incorporates all available chronological constraints including stratigraphic ordering, superposition, cross-cutting relationships, and historical data to trim the possible age range of a unit or event. The OxCal program also provides a quantitative means to identify and discard ages that are either too young or too old due to the introduction of these materials by bioturbation (but not recognized in the sampling process). This proportion of the research is still in progress since additional radiocarbon dates are forthcoming (NEHRP Grant 05HQGR0615).

Publications Resulting from this NEHRP Research:

Niemi, T.M., and Hall, N.T., submitted 2004, Paleoseismologic investigations of the northern San Andreas fault in Marin County, California, in GSA Special Volume, *Paleoseismology in the 21st Century—A Global Perspective*.

Grove, K., and Niemi, T.M., 2005, Late Quaternary deformation and slip rates in the northern San Andreas fault zone at Olema Valley, Marin County, California: *Tectonophysics*, v. 401, no. 3-4, p. 231-250.

Published Abstracts Related to this Contract:

Generaux, S., Niemi, T.M., Zhang, H., 2002, Historical pollen as an indicator for constraining earthquake stratigraphy along the San Andreas fault, Vedanta Marsh, Olema, CA (abst.): Annual Meeting, Geological Society of America, *Geological Society of America Abstracts with Program*, v. 34, no. 6, p. 27.

Generaux, S., Niemi, T.M., and Burns, R., 2003, Evidence for the Pleistocene-Holocene transition from a 20.8m core obtained from Vedanta Marsh, Olema, CA (abst.): North-Central Section Meeting of the Geological Society of America, Kansas City, MO, *Geological Society of America Abstract with Program*, v. 35 (2), p. 53.

Niemi, T.M., Zhang, H., Generaux, S., Fumal, T., and Seitz, G., 2002, A 2500-year Record of great earthquakes along the northern San Andreas fault at Vedanta marsh, Olema, CA (abst.): Cordilleran Section, *Geological Society of America Abstracts with Programs*, v. 34, no. 5, p. P-70.

Zhang, H., Niemi, T.M., Generaux, S., and Fumal, T., 2003, Earthquake events and recurrence interval on the northern San Andreas fault at Vedanta marsh site, Olema, CA (abst.): North-Central Section Meeting of the Geological Society of America, Kansas City, MO, *Geological Society of America Abstract with Program*, v. 35 (2), p. 58.

Zhang, H., Niemi, T.M., Generaux, S., Fumal, T., and Sietz, G., 2003, Paleoseismology of the Northern San Andreas fault at Vedanta marsh site, Olema, California (abst.): XVI International Quaternary Association Congress, Reno, NV, July 23-31, 2003.

References Cited

- Atwater, B., Hedel, C.W., Helley, E.J., 1977. Late Quaternary depositional history, Holocene sea-level changes, and vertical crustal movement, south San Francisco Bay, California. U.S. Geological Survey Professional Paper 1014. 15 pp.
- Bonilla, M.G. and Lienkaemper, J.J., 1990, Visibility of fault strands in exploratory trenches and timing of rupture events: *Geology*, v. 18, no. 2, p. 153-156.
- Clark, J.C., Brabb, E.E., 1997. Geology of Point Reyes National Seashore and vicinity: a digital database: U.S. Geological Survey Open-file Report 97-456, scale 1:48 000, 1 sheet. 17 p.
- Fumal, T.E., Weldon, R.J., Biasi, G.P., Dawson, T.E., Seitz, G.G., Frost, W.T., and Schwartz, D.P., 2002, Evidence for large earthquakes on the San Andreas fault at the Wrightwood, California, Paleoseismic site: A.D. 500 to Present: *Bulletin of the Seismological Society of America*, v. 92, no. 7, p. 2726-2760.
- Fumal, T., Pezzopane, S.K., Weldon, R.J., and Schwartz, D., 1993, A 100 year recurrence interval for the San Andreas fault at Wrightwood, California: *Science*, v. 259, p. 199-203.
- Galloway, A.J., 1977. Geology of the Point Reyes Peninsula, Marin County, California: *California Division of Mines and Geology Bulletin* 202, 72 pp.
- Generaux, S., Niemi, T.M., Zhang, H., 2002, Historical pollen as an indicator for constraining earthquake stratigraphy along the San Andreas fault, Vedanta Marsh, Olema, CA (abst.): Annual Meeting, Geological Society of America, *Geological Society of America Abstracts with Program*, v. 34, no. 6, p. 27.
- Gilbert, G.K., 1907a. The investigation of the California earthquake of 1906. In: *The California Earthquake of 1906*, D.S. Jordan, (Editor) and A.M. Robertson, San Francisco, 215-256.
- Gilbert, G.K., 1907b. The earthquake as a natural phenomenon, in The San Francisco earthquake and fire of April 18, 1906, and their effects on structures and structural materials: U.S. Geological Survey Bulletin 324, 1-13.
- Goldfinger, C., Nelson, C.H., Johnson, J.E., and the Shipboard Scientific Party, 2003, Holocene earthquake records from the Cascadia subduction zone and northern San Andreas fault based on precise dating of offshore turbidites: *Annual Reviews in Earth Planetary Sciences*, p. 31, 555-31, 577, doi: 10.1146/annurev.earth.31.100901.141246.
- Grove, K., and Niemi, T.M., 2005, Late Quaternary deformation and slip rates in the northern San Andreas fault zone at Olema Valley, Marin County, California: *Tectonophysics*, v. 401, no. 3-4, p. 231-250.
- Grove, K., Colson, K., Binkin, M., Dull, R., and Garrison, C., 1995, Stratigraphy and structure of the Late Pleistocene Olema Creek Formation, San Andreas fault zone north of San Francisco, California, in Sangines, E., Andersen, D., Buising, A., eds., *Recent Geologic Studies in the San Francisco Bay Area*: Society for Sedimentary Geology (SEPM) Pacific Section Book 76, p. 55-77.
- Hall, N.T., Wright, R.H., and Clahan, K.B., 1999, Paleoseismic studies of the San Francisco Peninsula segment of the San Andreas fault zone near Woodside, California: *Journal of Geophysical Research*, v. 104, p. 23,215-23,236.
- Hall, N.T., and Hughes, D.A., 1980, Quaternary geology of the San Andreas fault zone at Point Reyes National Seashore, Marin county, California, in Streitz, R., and

- Sherburne, R., eds., *Studies of the San Andreas fault zone in northern California*: California Division of Mines and Geology Special Report 140, p.71-87.
- Harris, R.A., and Simpson, R.W., 1998, Suppression of large earthquake by stress shadows: a comparison of Coulomb and rate-and-state failure: *Journal of Geophysical Research*, v. 103, p. 24,439-24,451.
- Kleist, J.R., (editor) 1981, The Franciscan Complex and the San Andreas fault from the Golden Gate to Point Reyes, California: Pacific Section, *American Association of Petroleum Geologists*, vol. 51, 31 p.
- Knudsen, K.L., Witter, R.C., Garrison-Laney, C.E., Baldwin, J.N., and Carver, G.A., 2002, Past earthquake-induced rapid subsidence along the northern San Andreas fault: A paleoseismological method for investigating strike-slip faults: *Bulletin of the Seismological Society of America*, v. 92, n. 7, p. 2612-2636.
- Lawson, A., 1908, *The California Earthquake of April 18, 1906*; Report of the State Earthquake Investigation Commission: Carnegie Institute Washington Publication 87, 451 pp. (Reprinted 1969).
- Niemi, T.M., Zhang, H., Generaux, S., Fumal, T., and Seitz, G., 2002, A 2500-year record of great earthquakes along the northern San Andreas fault at Vedanta marsh, Olema, CA (abst): Cordilleran Section meeting, *Geological Society of America Abstract with Programs*, v. 34, no. 5, p. P-70.
- Niemi, T.M., Zhang, H., Mansoor, N., Gierke, J.C., Hall, N. T., Wells, D.L., and Thronberg, J., 1999, Paleoequake chronology on the Northern San Andreas fault at the Vedanta Marsh Site, Marin County, California (abst): GSA Cordilleran Sec. *Abstracts with Programs*, v. 31 (6), p. A-83.
- Niemi, T.M., and Hall, N.T., 1996, Historical changes in the tidal marsh of Tomales Bay and Olema Creek, Marin County, California: *Journal of Coastal Research*, v. 12, no. 1, p. 90-102.
- Niemi, T.M., and Hall, N.T., 1992, Late Holocene slip rate and recurrence of great earthquakes on the San Andreas fault in northern California: *Geology*, v. 20, p. 195-198.
- Niemi, T.M., 1992, Late Holocene slip rate, prehistoric earthquakes, and Quaternary neotectonics of the Northern San Andreas fault in Marin County, California. Ph.D. dissertation, Stanford University, Stanford, CA, 6 Plates, 199 p.
- Noller, J.S., and Lightfoot, K.G., 1997, An archaeoseismic approach and method for the study of active strike-slip faults: *Geoarchaeology*, v. 12, p. 117-135.
- Ramsey, C. B., 2005, OxCal Program Ver. 3.10, Radiocarbon Accelerate Unit, University of Oxford, U.K. (http://units.ox.ac.uk/departments/rlaha/orau/06_01.htm)
- Schwartz, D.P., and Coppersmith, K.J., 1984, Fault behavior and characteristic earthquakes: Examples from the Wasatch and San Andreas fault Zones: *Journal of Geophysical Research*, v. 89, p. 5681-5698.
- Schwartz, D.P., Pantosti, D., Okumura, K., Powers, T.J., and Hamilton, J.C., 1998, Paleoseismic investigation in the Santa Cruz Mountains, CA-Implications for recurrence of large magnitude earthquakes on the San Andreas fault: *Journal of Geophysical Research*, v. 103 (B8), 17,985-18,001.
- Thatcher, W., Marshall, G., Lisowski, M. 1997, Resolution of fault slip along the 470-km-long rupture of the great 1906 San Francisco earthquake and its implications, *Journal of Geophysical Research*, v. 102, p. 5353-5467.

- Topozada, T.R., Branum, D.M., Reichle, M.S., and Hallstrom, C.L., 2002, San Andreas fault zone, California: $M \geq 5.5$ earthquake history: *Bulletin of the Seismological Society of America*, v. 92, no. 7, p. 2555-2601.
- Topozada, T.R. and Bortugno, E.J., 1998, Re-evaluation of the 1836 “Hayward fault” and the 1838 San Andreas fault earthquakes: *Bulletin of the Seismological Society of America*, v. 88, p. 140-159.
- Topozada, T.R., Real, C.R., Parke, D.L., 1981, Preparation of isoseismal maps and summaries of reported effects for pre-1906 California earthquakes: *California Division Mines and Geology Open-File Report 81-11*, 182 p.
- WGCEP, 2003, Summary of earthquake Probabilities in the San Francisco Bay region: 2002-2032: U. S. Geological Survey, Open-File Report 03-214.
- Weldon, R.J., McCalpin, J.P., and Rockwell, T.K., 1996, Chapter 6: Paleoseismology of strike-slip tectonic environments, in McCalpin, J.P. (ed.), *Paleoseismology*: NY, Academic Press, p. 271-329.
- Zhang, H., 2005, Paleoseismic Studies of the Northern San Andreas Fault at Vedanta Marsh Site, Olema, California: Interdisciplinary Ph.D. Dissertation, Department of Geoscience, University of Missouri-Kansas City.
- Zhang, H., Niemi, T. M., Generaux, S., and Fumal, T. E., 2003a, Earthquake events and recurrence interval on the northern San Andreas fault at Vedanta marsh site, Olema, CA: North-Central Section Meeting, Geological Society of America, Kansas City, MO, *GSA Abstracts with Programs*, v. 35 (2), p. A-58.
- Zhang, H., Niemi, T. M., Generaux, S., Fumal, T. E. and Seitz, G., 2003b, Paleoseismology of the northern San Andreas fault at Vedanta marsh site, Olema, CA: the XVI International Quaternary Association Congress, Reno, NV, *INQUA Abstracts with Programs*, p.107.
- Zoback, M. L., and Schwartz, D.P., 1999, San Andreas-San Gregorio fault source characterization as input into earthquake probabilities (abst.): *GSA Abstracts with Programs*, v. 31(6), p. A-113.

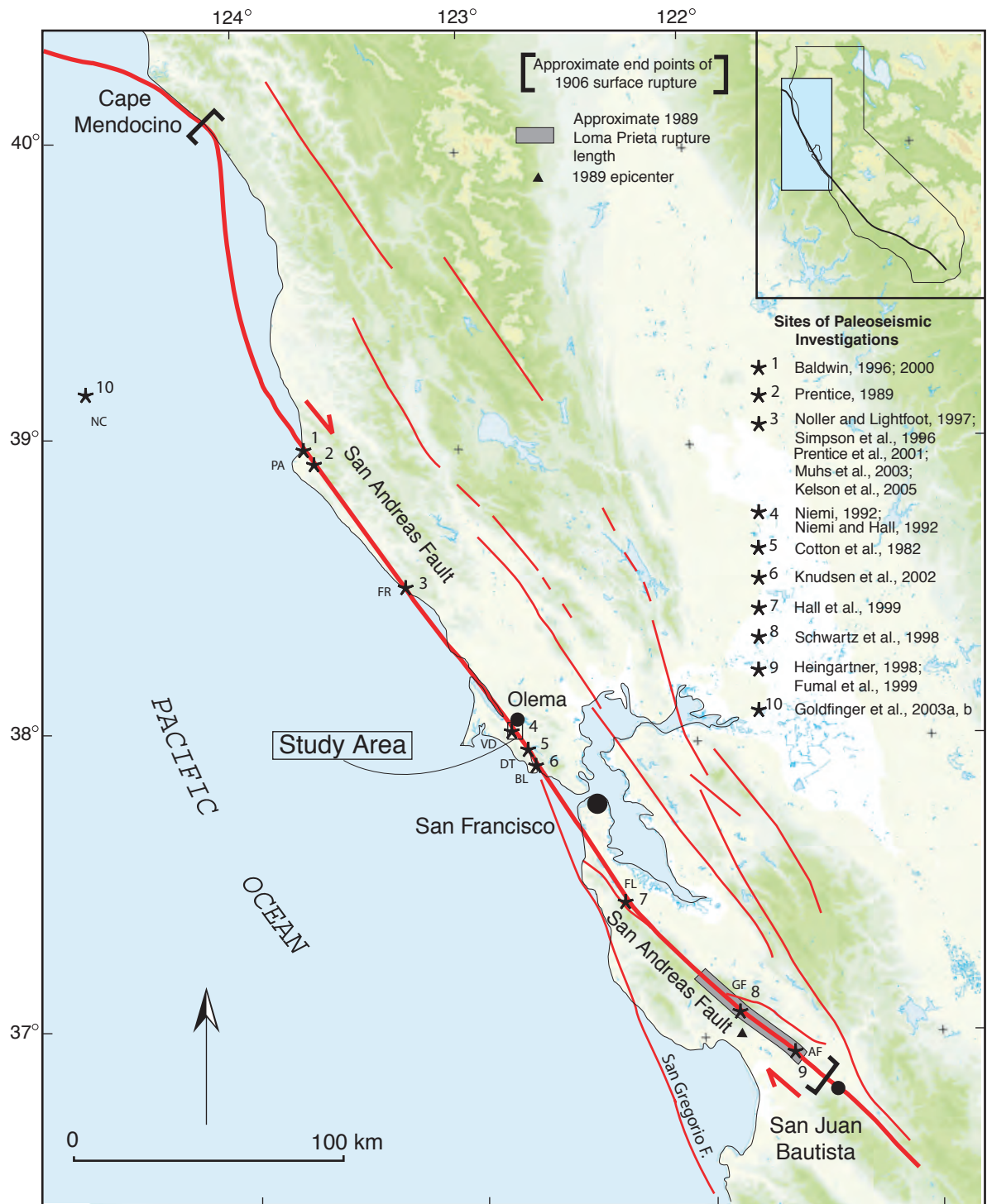


Figure 1. Map of the Bay Area showing the major faults and locations of paleoseismic sites along the northern San Andreas fault. Asterics denote paleoseismic sites. PA, Point Arena; FR, Fort Ross; VD, Vedanta; DT, Dogtown; BL, Bolinas; FL, Filoli; GF, Grizzly Flat; AF, Arano Flat; NC, Noyo Channel.

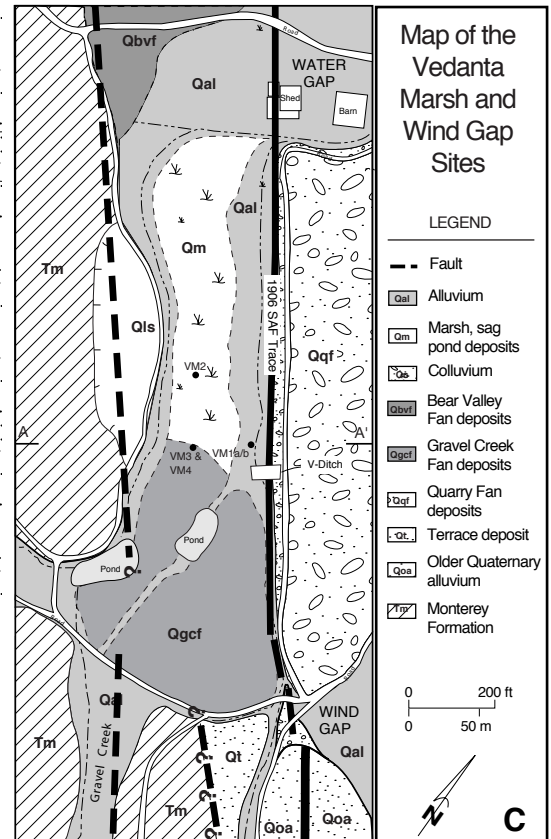
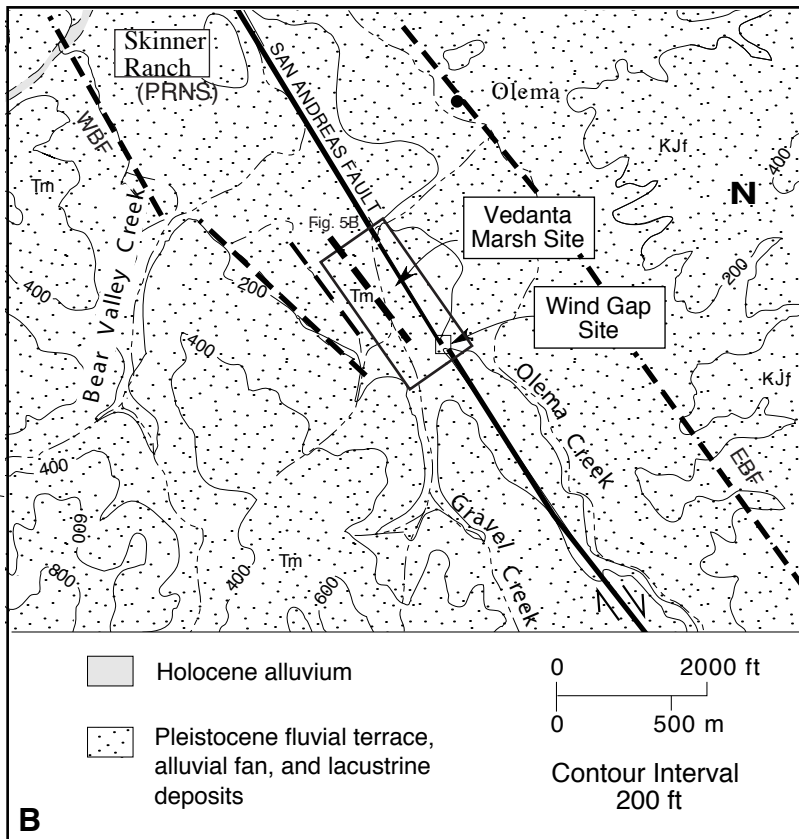
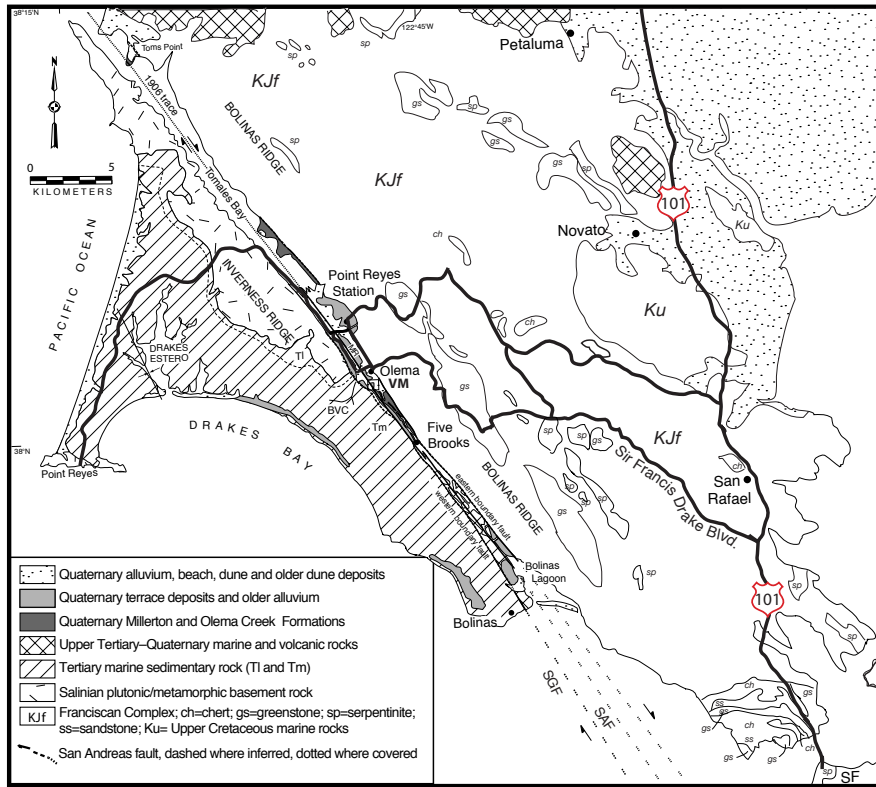


Figure 2:A) Geologic map of Marin County. MR = medial ridge. BVC = Bear Valley Creek drainage. [Map modified from Galloway (1977); Kleist (1981); Clark and Brabb (1997)] B) Map of Olema Valley showing location of the marsh and wind gap research sites with contours from U.S. Geological Survey 7.5-minute Inverness quadrangle. PRNS = Point Reyes National Seashore headquarters. EBF = East boundary fault. WBF = West boundary fault. C) Surficial geologic map of the Vedanta marsh showing the location of paleoseismic trenches that have been excavated across the San Andreas fault at this site.

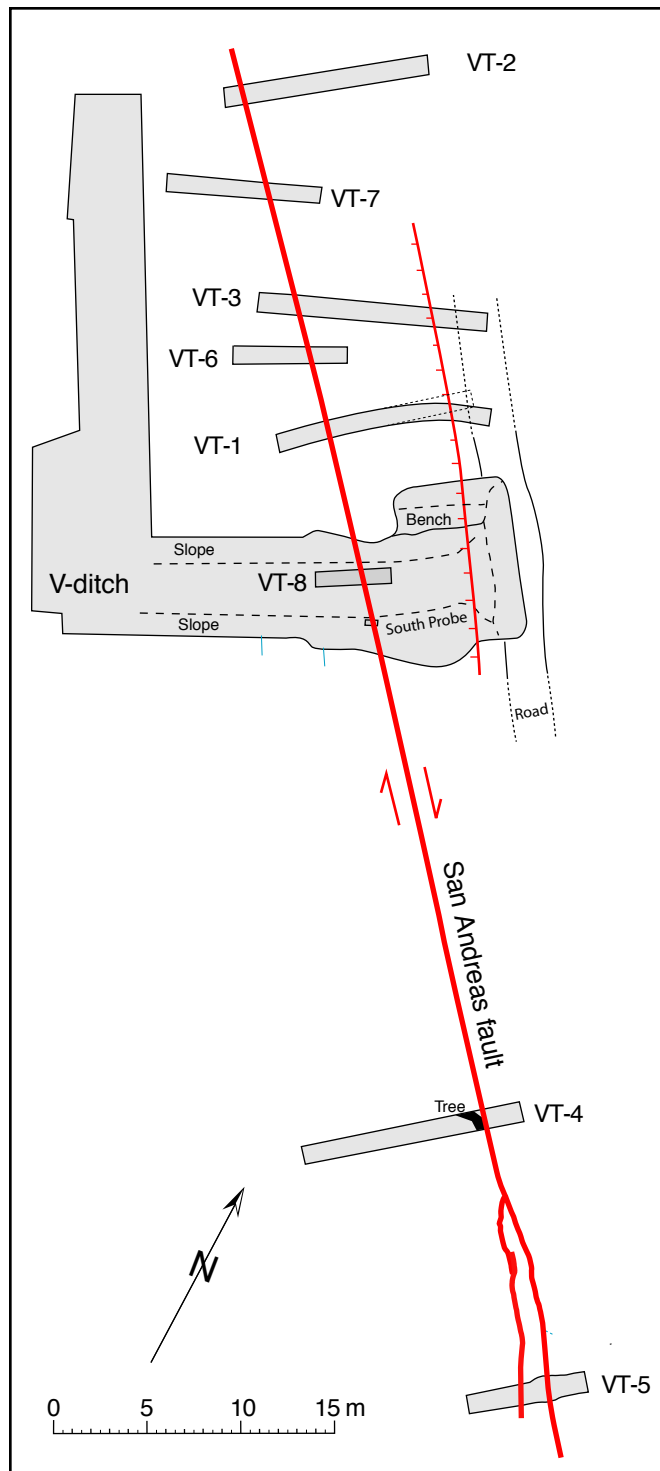


Figure 3: Map of the paleoseismic trenches at the Vedanta marsh site.

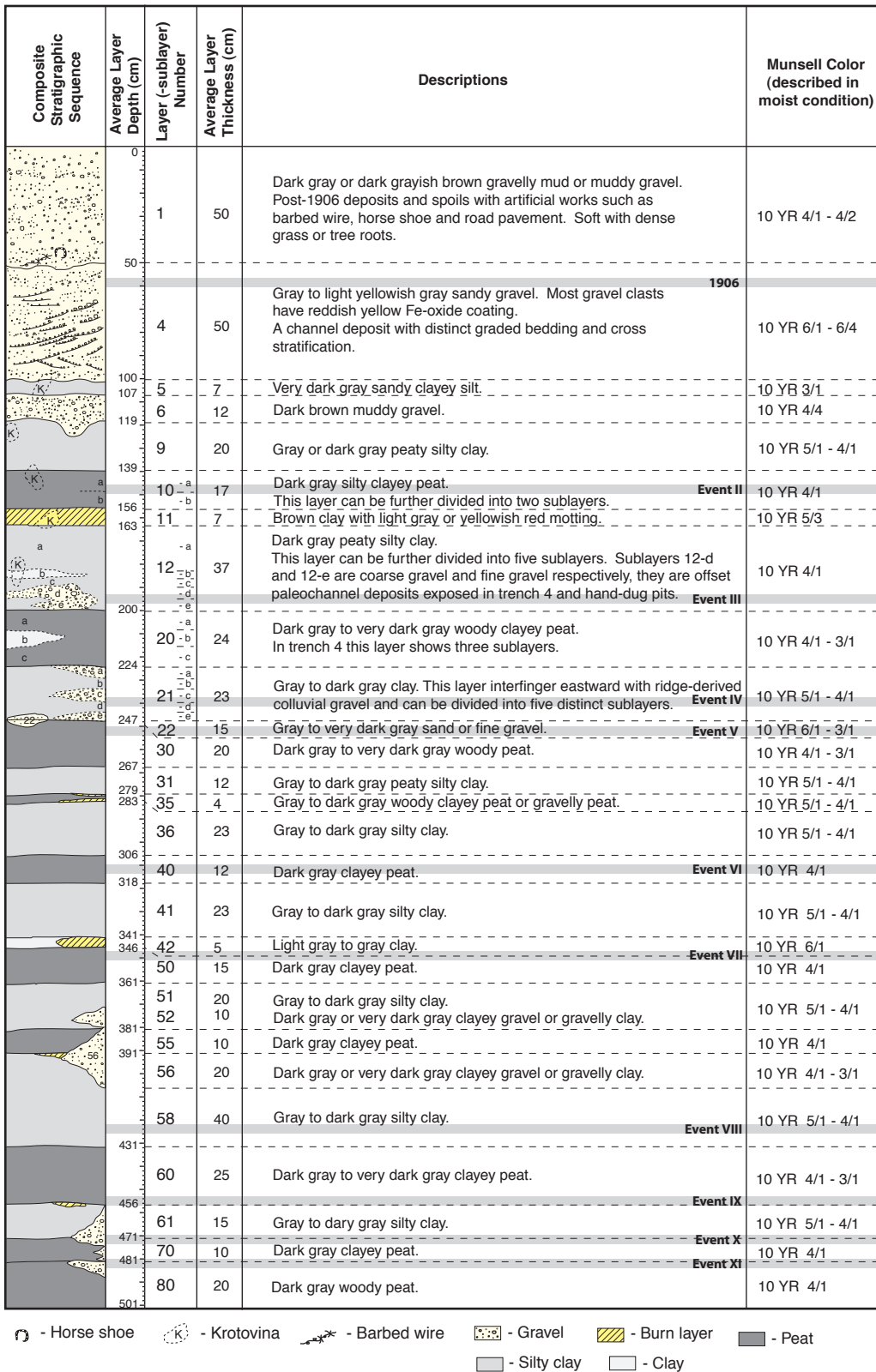


Figure 4: Generalized stratigraphic column of the section exposed by the excavations.

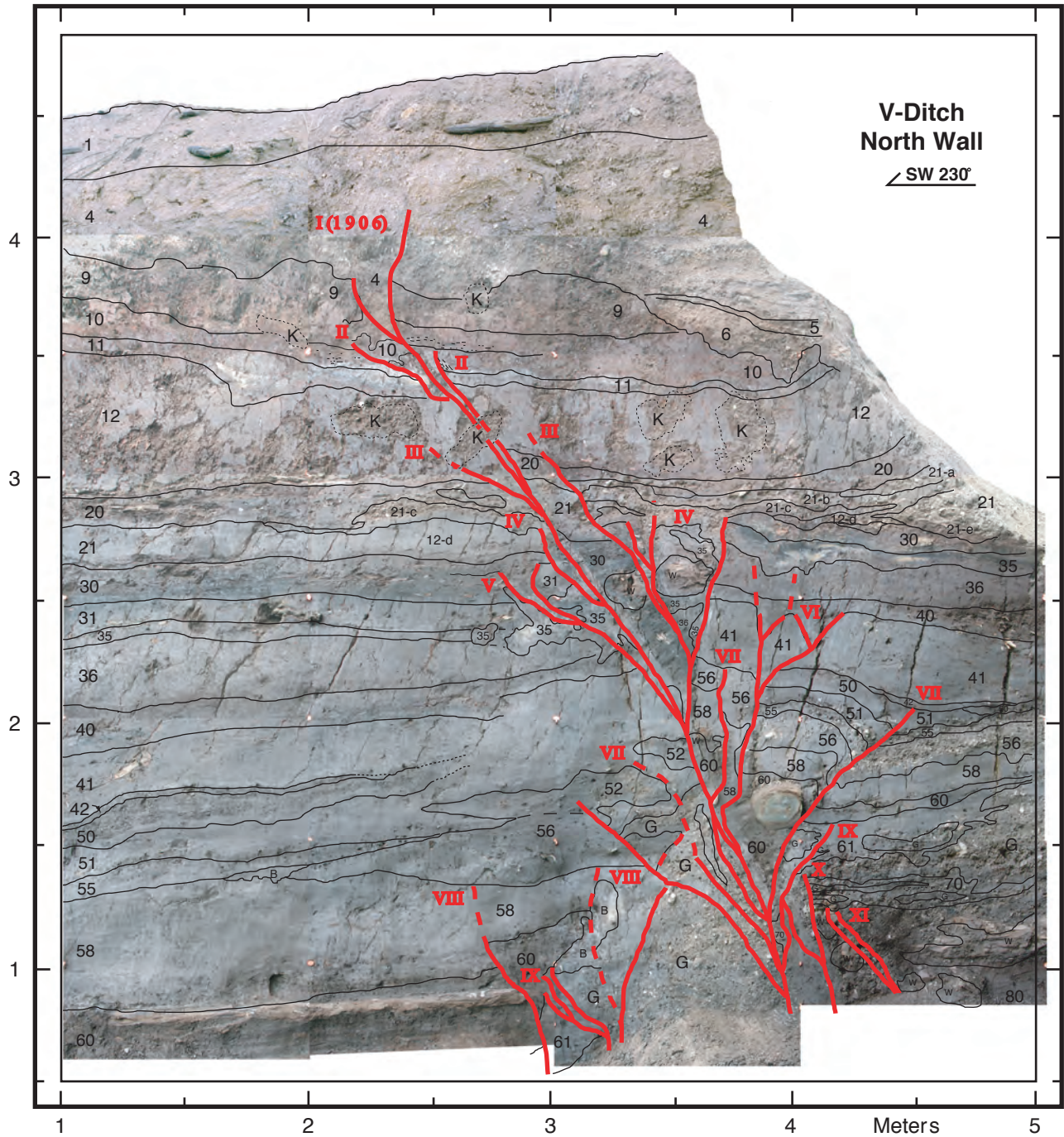


Figure 6: Photomosaic and trench log of the north wall of the V-Ditch showing evidence for eleven earthquakes over the past 2500 years.

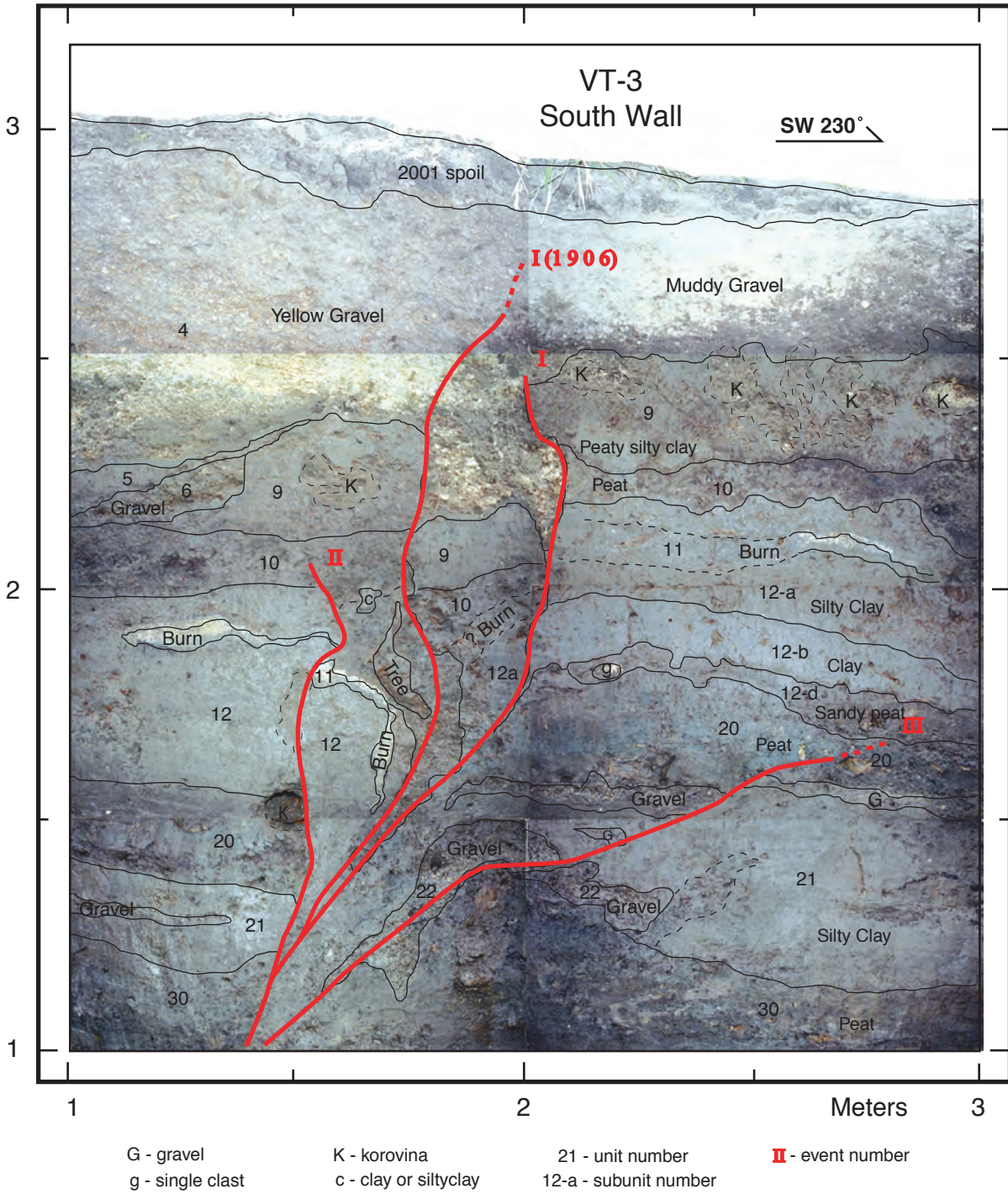


Figure 7: Evidence for the three most recent earthquakes (Events I-III) in the south wall of Trench VT-3. Photomosaic and Log from 06-14-2002. (Modified from H. Zhang, 2005).

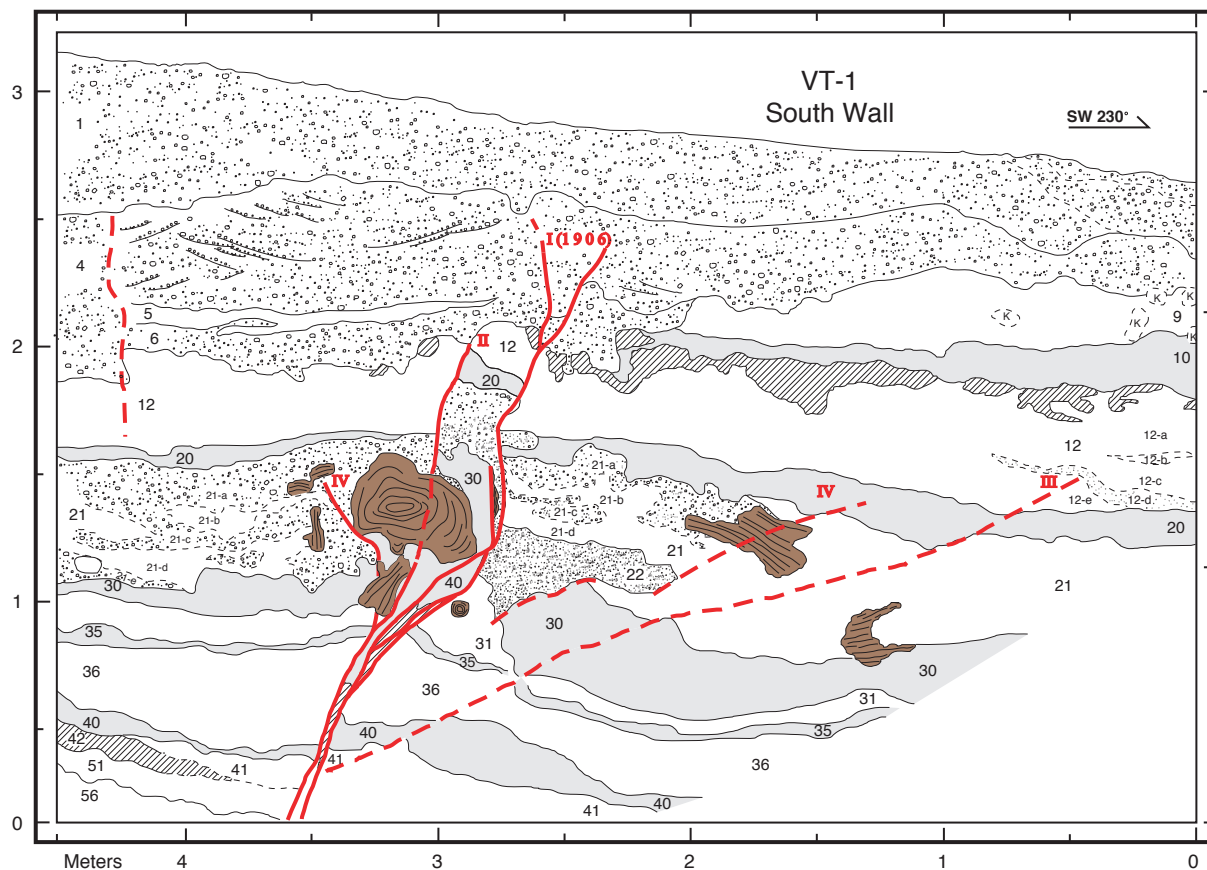


Figure 8: Graphic log of the south wall of Trench VT-1 along the main fault zone. (Modified from H. Zhang, 2005).

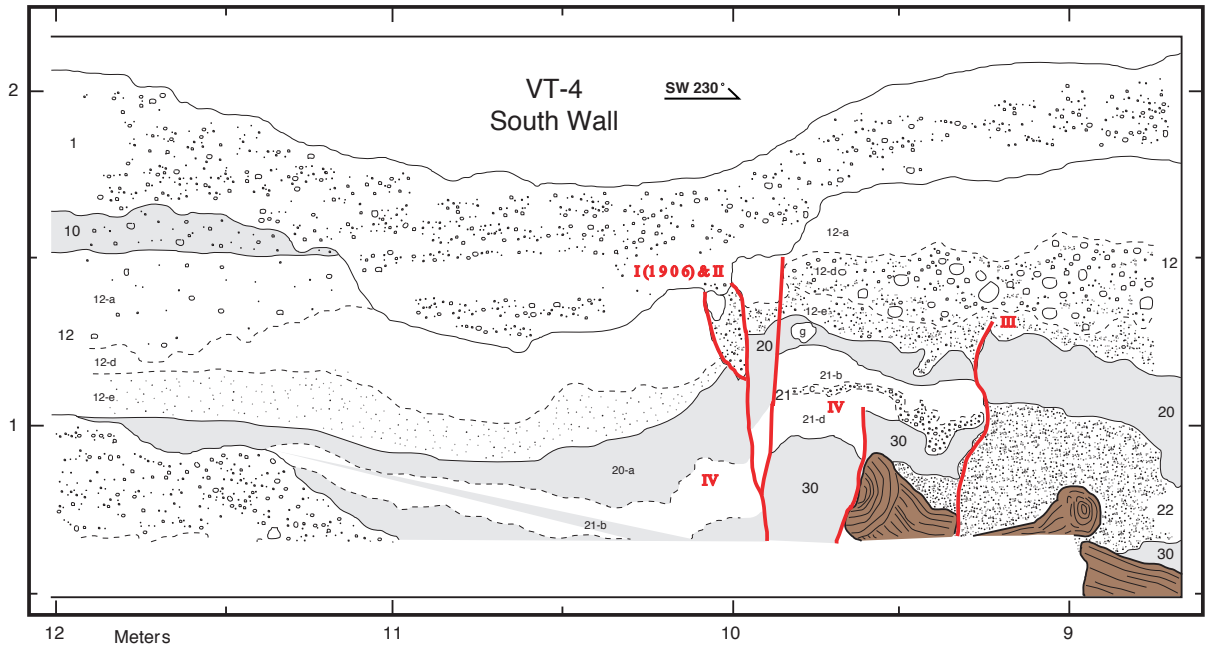


Figure 9: Graphic log of a portion of the south wall of Trench VT-4.

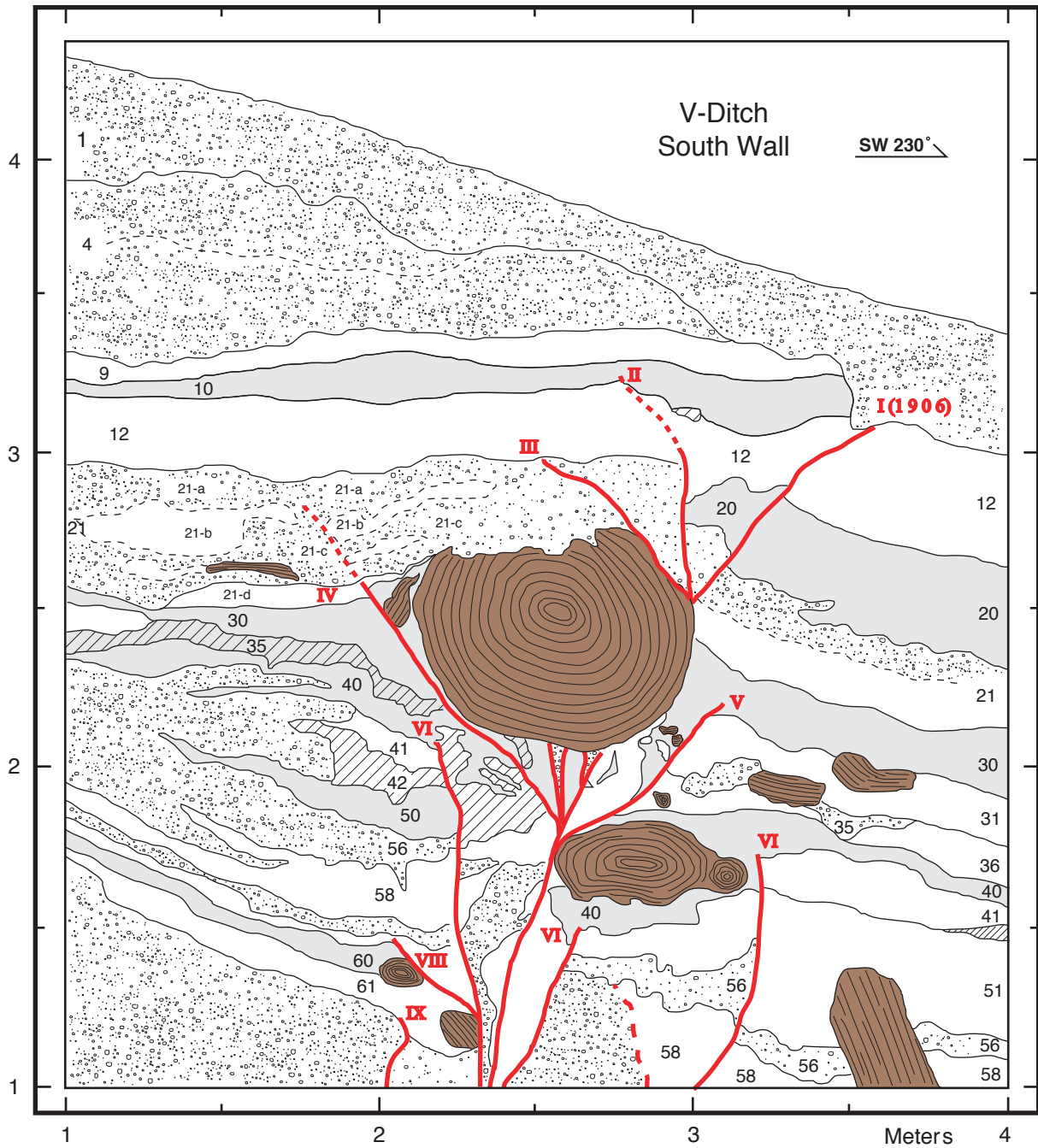


Figure 10: Trench log of the south wall of the V-Ditch at the main fault zone in 2001 & 2002.

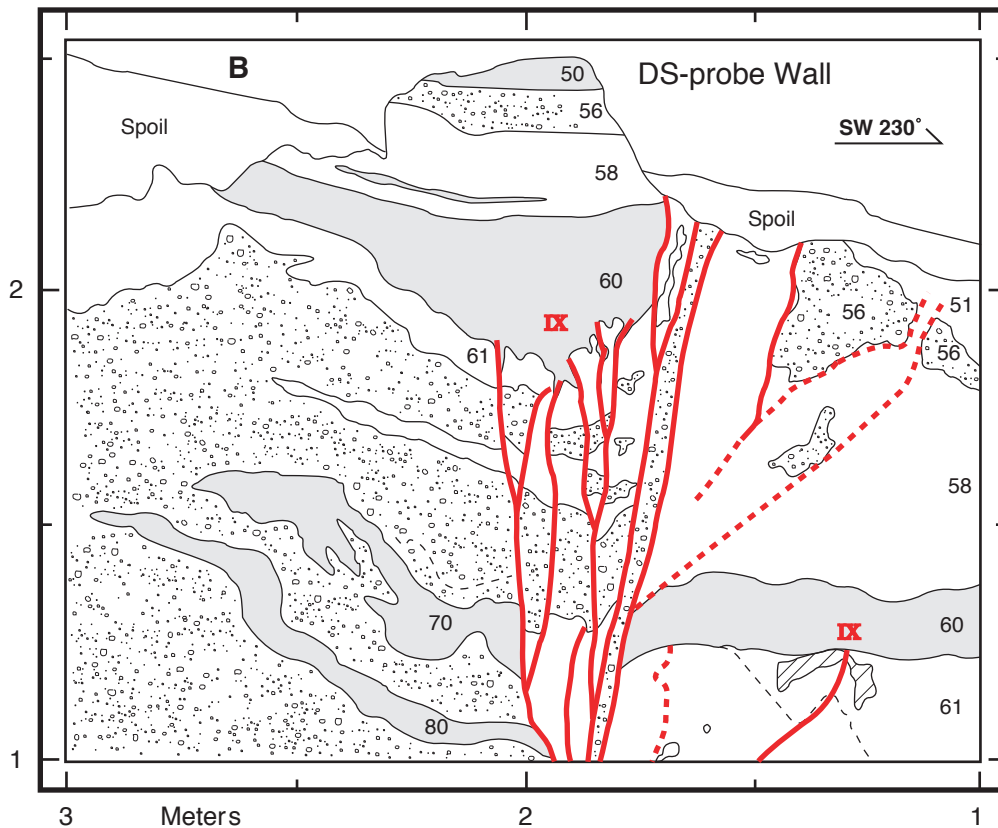
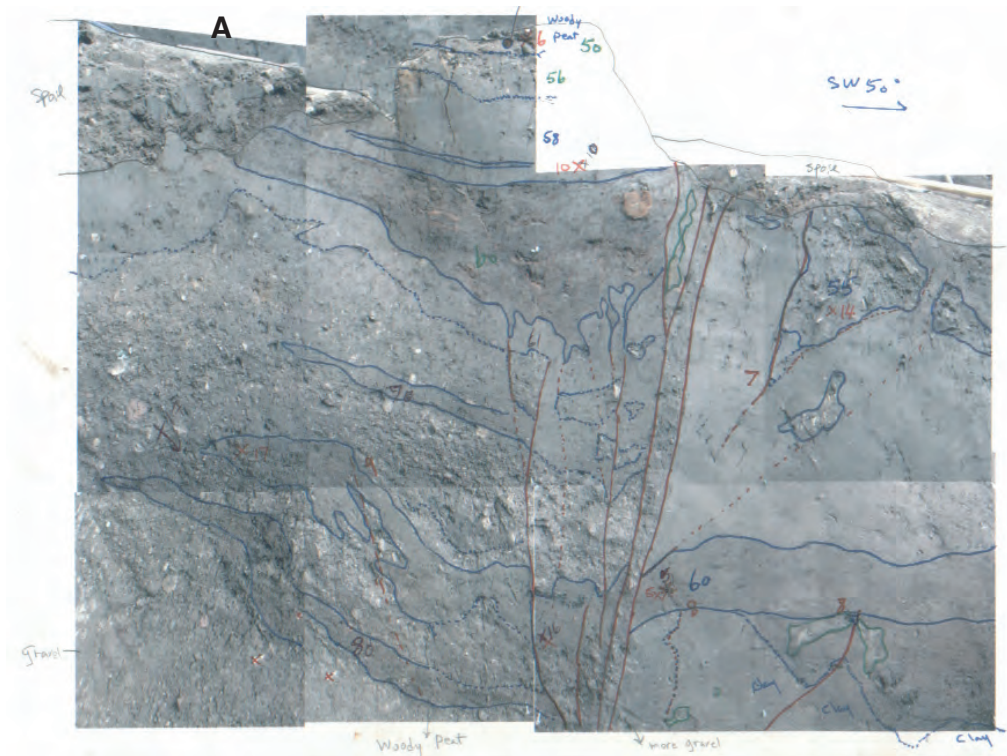


Figure 11: Trench log of the DS-probe wall, a hand-dug pit located 1.5 m northwest of the south wall of the V-Ditch. Exposure dug and mapped in July, 2002. (Zhang, 2005).

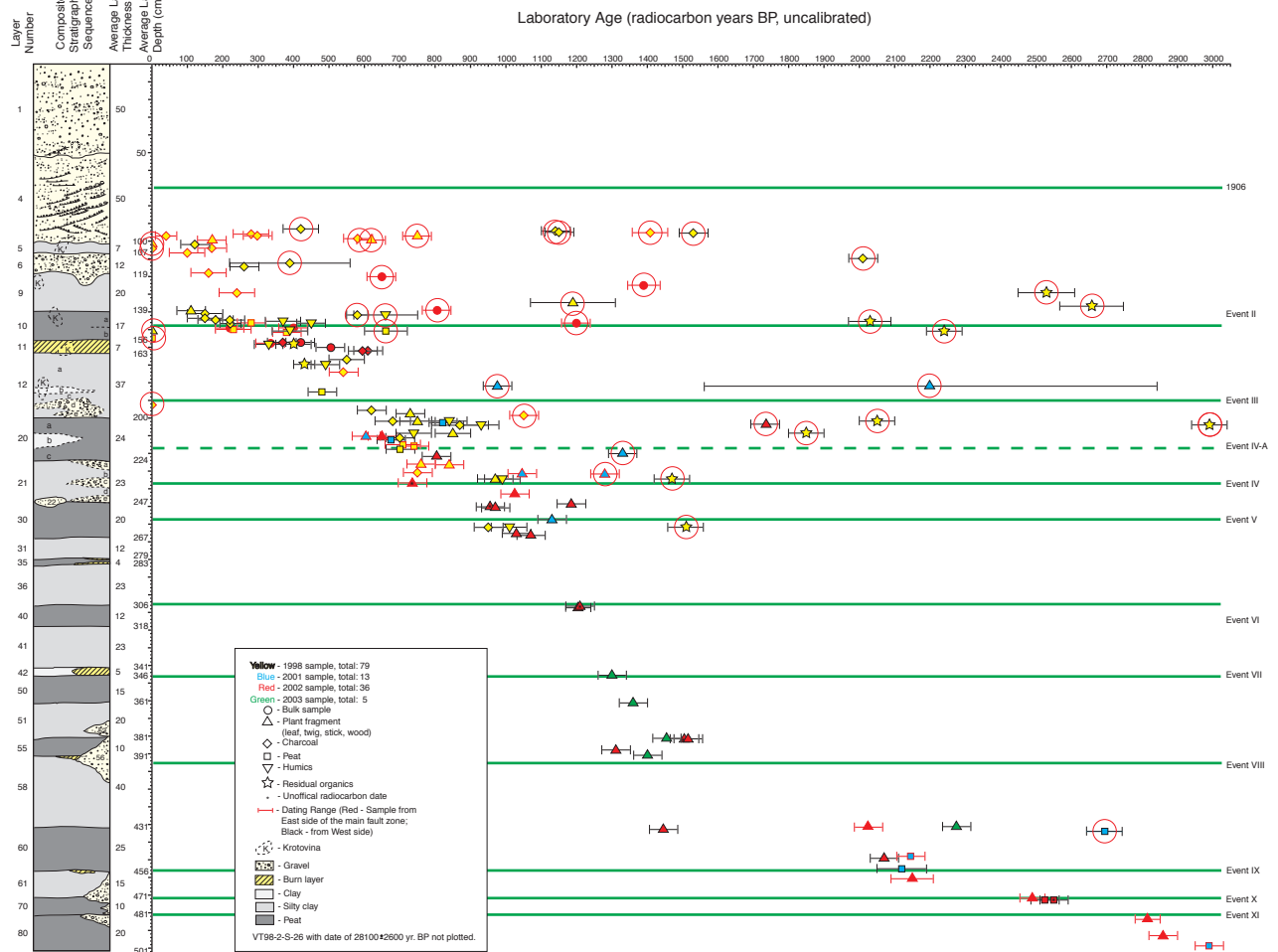


Figure 12: Scatter plot of uncalibrated radiocarbon ages for dated samples versus stratigraphic sequence by depth below the ground surface. Horizontal bars indicate the uncertainty of the age determination. The position of each event horizon relative to the stratigraphic level are shown with a green line (Modified after Zhang, 2005).